



Original articles

Research article

<https://doi.org/10.17308/kcmf.2024.26/12219>

Formation of smooth and microporous ZnO-based substrate material

A. M. Ismailov¹✉, A. E. Muslimov²

¹Dagestan State University,
43-a Magomet Gadzhiev st., Makhachkala 367000, Republic of Dagestan, Russian Federation

²National Research Centre “Kurchatov Institute”
1 Akademika Kurchatova pl., Moscow 123182, Russian Federation

Abstract

The paper investigates the influence of the deposition temperature on the morphology and structural-phase composition of the ZnO-based substrate material with a thickness of over 50 μm during the magnetron sputtering of hot ceramic targets.

The study revealed the influence of the deposition temperature on the growth rate, morphology, and structural parameters of the ZnO single crystal precipitate. It was shown that the ZnO deposition rates during the spluttering of hot ceramic targets were ultra-high (up to 1.5 μm/min). The authors propose a method for the formation of both smooth and microporous ZnO-based substrate materials without using template technologies.

The results obtained in the work can be widely used in optoelectronics and nitride technologies.

Keywords: Zinc oxide, Hot target, Magnetron sputtering, Microporous Structure, substrates, Nitride technologies

Funding: This study was supported by Russian Science Foundation (grant No. 24-29-00696).

For citation: Ismailov A. M., Muslimov A. E. Formation of smooth and microporous ZnO-based substrate material *Condensed Matter and Interphases*. 2024;25(3): 440–446. <https://doi.org/10.17308/kcmf.2024.26/12219>

Для цитирования: Исмаилов А. М., Муслимов А. Э. Формирование гладкого и микропористого подложечного материала на основе ZnO. *Конденсированные среды и межфазные границы*. 2024;26(3): 440–446. <https://doi.org/10.17308/kcmf.2024.26/12219>

✉ Ismailov Abubakar Magomedovich, e-mail: egdada@mail.ru

© Ismailov A. M., Muslimov A. E., 2024



The content is available under Creative Commons Attribution 4.0 License.

1. Introduction

Many modern optoelectronic devices, in particular white LEDs, are based on nitride technologies. The main components of white LEDs are blue-light emitting LEDs [1,2] and phosphors that convert blue-light quanta into quanta of lower energy [3, 4]. A typical example of a blue LED is the multi-layer InGaN/GaN heterostructure with an active region based on multiple InGaN quantum wells [5]. Significant disadvantages of such structures reducing the light yield efficiency are background impurities, high density of lattice defects, and mechanical stresses affecting the parameters of the band structure. Structural defects and stresses are associated with discrepancies between the crystallographic parameters of nitride growth structures and sapphire substrates. Also, total internal reflection leading to photon scattering results in a decrease in the efficiency of light-emitting devices. Background impurities are almost impossible to eliminate due to the specific features of the method of organometallic vapor-phase epitaxy, while defects and stresses can be reduced by using “native” substrates for nitride compounds. Currently, widespread use of “native” gallium nitride substrates is not possible due to their high production costs. Therefore, it appears to be promising to use a ZnO-based substrate material (a gallium nitride isostructural material). Despite the minimal discrepancies between the parameters of ZnO and GaN (less than 2% [6]), the production of bulk ZnO single crystals is also expensive, however, ZnO film synthesis technologies are simple and affordable. To use ZnO films as a substrate material, their sufficient thickness should be at least tens of micrometers. Conventional thin-film technologies for gas-phase, magnetron deposition, laser ablation, etc. are characterized by relatively low growth rates and are not designed to produce bulk substrate material.

In this paper, the technology of magnetron sputtering of hot zinc oxide ceramic targets was used to obtain thick ZnO layers, i.e. a ZnO target, thermally insulated from the water-cooled magnetron base, was sputtered. It should be noted that the hot sputtering technology is mainly used for sputtering single-component metal targets [7,8]. In addition, it is known [9] that

oxide or nitride films are formed by sputtering hot metal targets in the corresponding gaseous medium. In this regard, studies dedicated to the sputtering of multicomponent ceramic targets at a high discharge power are very relevant. The main problem is associated with the difficulty of building a model for sputtering of “hot” ceramic targets. In contrast to the cooled target sputtering, cascade sputtering is accompanied by interconnected processes of radiation-enhanced diffusion of atoms, leading to the formation of growths on the surface of the target, and microparticle emissions characteristic of shock-evaporation processes. Due to the inhomogeneity of the gas phase, the study of deposition processes and their dependence on technological parameters (discharge power, pressure of the working gas, and substrate temperature) is important and of scientific novelty. It is challenging to consider all parameters at the same time, so at this stage only the temperature of the substrate was changed. Our first results on the sputtering of hot ZnO ceramic targets were published earlier [10]. Studies showed that at a sufficiently high temperature of the substrate of 900 °C, epitaxial films were formed with an ultra-high rate of about 0.9 $\mu\text{m}/\text{min}$, which is uncommon for thin-film technologies. What is more, the films had a developed micromorphology and characteristic hexagonal microcrystals up to several micrometers in size were isolated on the surface. It should be noted that reducing the deposition temperature is a priority that meets the requirements of energy efficiency. A decrease in the deposition temperature under conditions of high discharge power and, as a result, high inhomogeneity of the ionized gas phase, can lead to radical changes in the growth processes. This work studies the influence of the deposition temperature on the morphology and structural-phase composition of the ZnO-based substrate material with a thickness of more than 50 μm during the magnetron sputtering of hot ceramic targets.

2. Experimental

Chemically and mechanically polished R-plane of a sapphire was used as a substrate. ZnO films were precipitated by magnetron sputtering with a cut-off of the cooling mode as described in [10], under the following conditions:

type I: temperature 750 °C, oxygen atmosphere, pressure 1 Pa, discharge current strength 500 mA, deposition time 35 min; type II: temperature 830 °C, oxygen atmosphere, pressure 1 Pa, discharge current strength 500 mA, deposition time 2 h. Samples obtained at a temperature of 900 °C (type III) were used for comparison [10].

X-ray diffraction (XRD) was used for structural studies of the films. X-ray diffraction patterns were recorded with Bragg-Brentano geometry using an Empyrean diffractometer manufactured by PANalytical (Netherlands). The study involved using copper anode radiation ($\text{CuK}\alpha_2 = 1.54 \text{ \AA}$). Electron microscopic studies of the cross-section of the sample were carried out on a Jeol NEOSCOPE 2 (JCM-6000) scanning electron microscope (SEM).

3. Results and discussion

During the hot ceramic target sputtering, the target is heated, which results in the formation of growths of various morphologies on the target surface. These growths are further destroyed by micro-arcs, as a result of which both ionized components and their microparticles enter the gas phase. The large mass of the microparticles restricts their diffusion activity on the growing surface. In addition, it is necessary to take into consideration that the adsorbed microparticles can melt. The melting point in thin layers is lower, and the Tammann temperature (T_t) can be used as a rough estimate [11]: $T_t \approx (0.3-0.5) T_0$, where $T_0 = 1,975 \text{ °C}$, the melting point of bulk ZnO. The vibration spectrum of the atoms on the crystal surface differs from their bulk spectrum. The oscillation amplitude of atoms located on the surface is always much higher than in bulk. It was established that for a wide class of single crystals of metals and semiconductors, the Debye temperature T_D , at which all vibrational modes in a solid are excited, for the surface phase, decreases to the values of about $0.5 T_D$ [12]. For ZnO, the value of T_D is about 100 °C [13] and at low temperatures, a significant weakening of the elastic harmonic forces in the near-surface layers of ZnO can be expected. Therefore, at the precipitation temperatures of 700–900 °C studied in the work, the processes of precipitate nucleation and growth cardinally depended on the temperature of the substrate.

The thickness of the ZnO film on the *R-plane* of the sapphire measured by SEM was 53.6 μm . The average growth rate of ZnO films was about 1.50 $\mu\text{m}/\text{min}$, which is a high rate comparable to the growth rate of ZnO uniaxial microcrystals (monocrystalline whiskers). The high rate was achieved due to the emission of microparticles from the surface of the hot target and their incorporation in a growing film according to the “liquid-crystal” mechanism [10]. The surface of the ZnO film was rough and morphologically heterogeneous (Fig. 1a) with individual microcrystallites of different shapes.

During the next stage, the ZnO film easily separated from the sapphire substrate. This was facilitated by a significant (more than 10 times) difference in the coefficients of thermal expansion of ZnO and sapphire and a sufficiently large thickness of the ZnO film. According to the SEM data, the lower (reverse) surface of the film (Fig. 1b) adjacent to the surface of the substrate during growth was cardinally different from the upper surface, which was loose. The lower surface was a honeycomb-like structure with linear sizes of its pores of 3–10 μm and a depth of up to 5 μm . The thickness of the pore walls was several micrometers (1–2 μm), which allows characterizing them as microwalls. The pore shape was predominantly trigonal. There were fewer pores of hexagonal shape and they were often compressed along one of the diameters of the hexagon. In addition, the microwalls had a multilayer structure.

The diffraction reflections in the XRD images (Fig. 2a) corresponded to the hexagonal (wurtzite) phase of ZnO (JCPDS card. No 36-1451). The ZnO film on both front and back sides was textured along direction [0001]. The XRD curve recorded on the back of the film had reflections associated with parasitic [103] crystallites. The parameters of the ZnO lattice calculated from the XRD data differed significantly for the two sides of the film. Parameters $d_{001} = 2.61 \text{ \AA}$ and $d_{103} = 1.48 \text{ \AA}$ for the porous part of the film were close to the standard ($d_{001} = 2.60 \text{ \AA}$ and $d_{103} = 1.477 \text{ \AA}$). Taking into consideration the low-intensity asymmetric reflexes on the diffraction pattern of the smooth front side of the film, parameters $d_{001} = 2.56 \text{ \AA}$ and $d_{110} = 1.610 \text{ \AA}$ were calculated, which appeared to be smaller than the standard ($d_{001} = 2.60 \text{ \AA}$ and

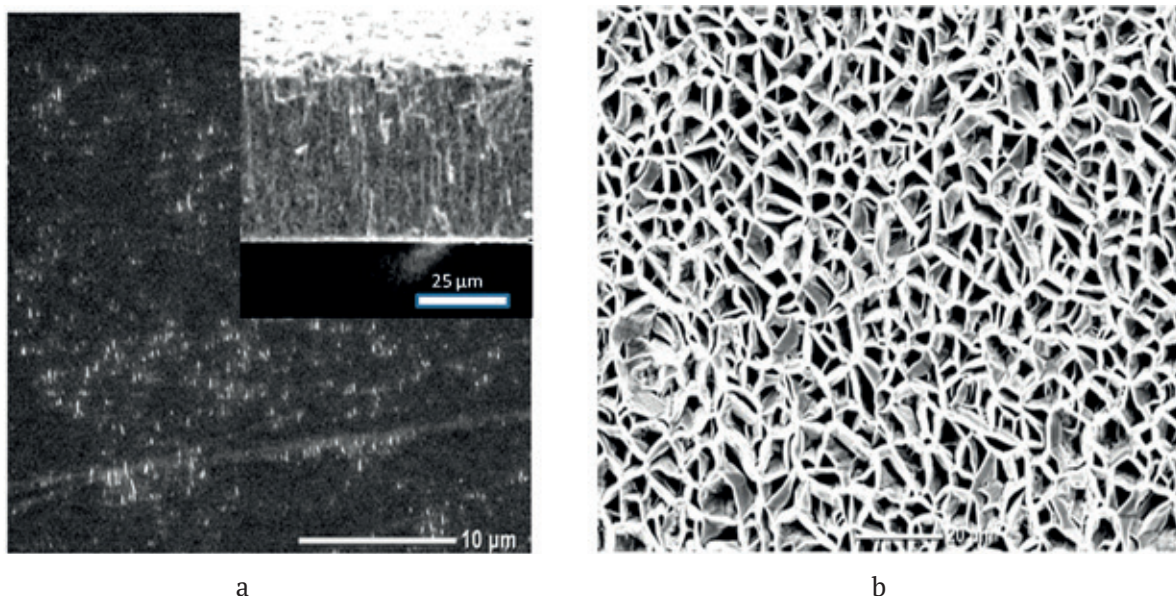


Fig. 1 Electron microscopic images of ZnO type I film: upper (a) and lower (b) surfaces

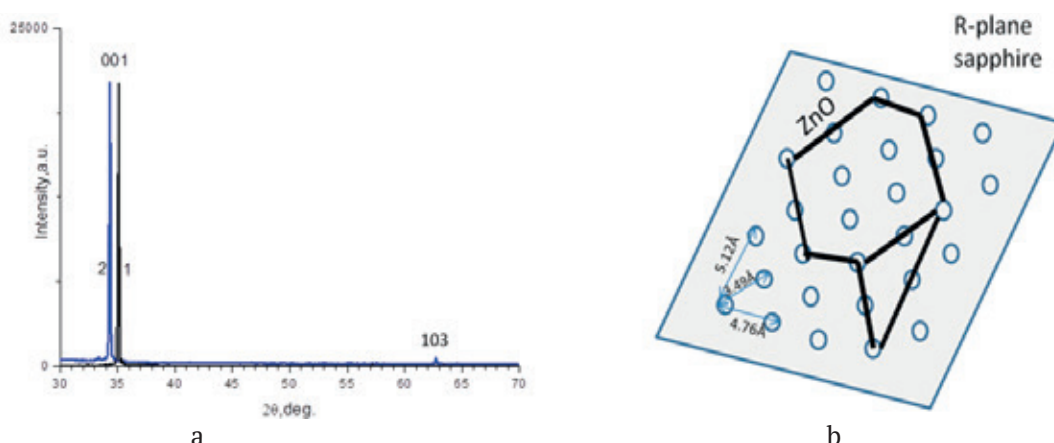


Fig. 2. a – X-ray diffraction patterns recorded from the upper (curve 1) and lower (curve 2) sides of the type I ZnO. b – scheme of the initial ZnO layers growth on the *R*-plane of the sapphire

$d_{110} = 1.6245 \text{ \AA}$). The unit cell volume $V = 45.97 \text{ \AA}^3$ was also smaller than the unit cell volume of the standard $V = 47.58 \text{ \AA}^3$, however, the decrease was mainly due to compression along axis $\langle 0001 \rangle$.

During the epitaxial deposition of ZnO on the *R*-plane of the sapphire, due to the structural and geometric similarity of the lattices, the following epitaxial ratio is usually realized: $A(110)\text{ZnO} \parallel R\text{-sapphire}$, with ZnO axis $[001]$ located in the plane of the sapphire surface [14]. In our case, $[110]$ -oriented ZnO crystallites were absent due to the specific features of hot target sputtering (emission of microparticles) and the peculiarities of nucleation at low diffusion mobility of clusters. The ZnO film was growing along energetically

favorable direction $[001]$. It is known [15] that $[001]$ -textured ZnO films grow quite easily even on non-orienting substrates. Parasitic $[103]$ crystallites of ZnO are usually observed in films growing at high rate [16]. The ZnO hexagonal structure of the wurtzite type had a six-fold symmetry. This was due to the formation of hexagonal and trigonal pores. ZnO clusters deposited on the *R*-plane of the sapphire self-organized along the directions with the highest linear density of atoms and in accordance with the symmetry of the wurtzite structure (Fig. 2b). What is more, the lattice points formed a rectangle (almost a square) with sides of 4.76 and 5.12 \AA , which explains the distortions of the

shape of the growing hexagonal and trigonal ZnO structures. Thus the first layer was formed and the subsequent ones were deposited on the previous one, forming a multilayer structure of the pore walls. It should be noted that the lattice parameters complied with the standard. The resulting honeycomb-like microstructure of the film confirmed a predominant emission of clusters from the surface of the overheated ZnO target. Adsorbed atoms and clusters, due to their diffusion activity, formed a continuous precipitate. The self-organization of ZnO microparticles on the sapphire surface must be mostly due to their Coulomb interaction, however, this needs to be studied in more detail.

The situation was different for the front side of the film. A significant compression of the Zn lattice and high stresses combined with the visually orange-brownish coloring of the film indicated a high concentration of structural defects, in particular oxygen vacancies. There was a high likelihood of oxygen deficiency in the clusters emitted by the target. Since a significant compression of the lattice was observed along axis $\langle 0001 \rangle$, it can be assumed that the ultra-high growth rate of ZnO films was due to the layering of oxygen-deficient clusters and the lag in the ordering process. Whereas a small deviation in azimuthal parameter α was associated with the high lateral activity of adatoms and clusters, supported by the high temperature of the substrate, which contributed to the partial filling of oxygen vacancies, interatomic interaction, and ordering.

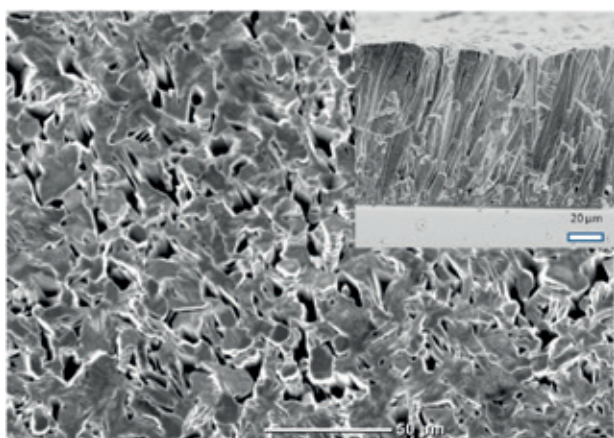


Fig. 3 Electron microscopic images of ZnO type II film

With an increase in the deposition temperature to 830 °C, the growth rate decreased to 0.85 $\mu\text{m}/\text{min}$. According to the SEM data, the thickness of the sample was 102 μm . The film had good adhesion to the substrate and did not peel off. The study of the morphology of the film section confirmed the columnar microstructure characteristic of ZnO synthesized at a high rate. The axis of the columnar microstructure deviated from the normal to the substrate plane, which was obviously associated with the direction of the shortest distance to the source (target). On the surface (Fig. 3) and in the film's bulk, there were penetrating micropores with a diameter of up to 10 μm . The elements of the columnar structure were formed by flat ZnO c -crystallites layered on top of each other. The high intensity of the incoming clusters created conditions in which, as a whole, the normal [17] growth of the ZnO precipitate prevailed. What is more, the formation of faceted flat microcrystals indicated a sufficient temperature for epitaxial deposition. However, there were no direct indicators of cluster melting at the adsorption stage.

According to X-ray diffraction data, a highly textured c -oriented ZnO film was formed during the deposition process. The parameters $d_{001} = 2.61 \text{ \AA}$ of the ZnO type II film were close to the standard ($d_{001} = 2.60 \text{ \AA}$). After the chemical-mechanical polishing, the surface of the ZnO film was smoothed to roughness values below 5 nm (Fig. 4). During the treatment, about 20 μm was stripped. The porosity remained at the level of

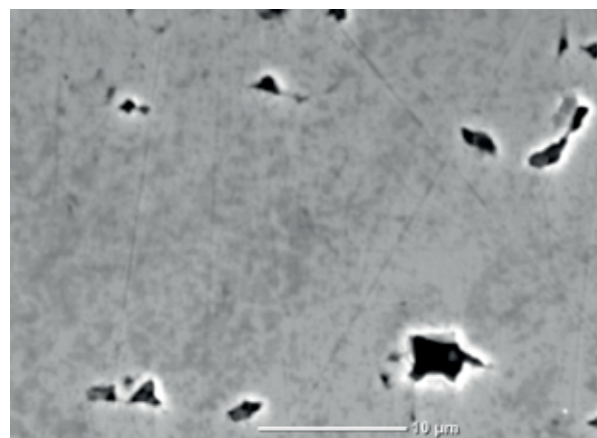


Fig. 4. Electron microscopic image of the surface of the ZnO type II film after chemical-mechanical polishing

10^6 cm^{-1} , which confirms the penetration of pores into the film bulk.

For comparison, the average growth rate of the type III film [10] was about $0.9 \mu\text{m}/\text{min}$. It can be concluded that after the deposition temperature was increased to above $800 \text{ }^\circ\text{C}$, the growth rate practically did not change. At these temperatures, the quality of the ZnO film was significantly improved, and the mechanisms of epitaxial deposition, azimuthal orientation of clusters were triggered. However, at higher temperatures, there were signs of cluster melting. Apparently, the deposited clusters came into thermal equilibrium with the substrate. The formation of hexagonal microparticles indicated that the crystallization mechanism proceeded under equilibrium conditions through the liquid phase of the initial microparticles melting. A decrease in the porosity of films at high deposition temperatures may also be associated with melting processes.

4. Conclusions

The paper investigated the influence of the deposition temperature during the magnetron sputtering of hot ZnO targets on the morphology and structural-phase composition of the ZnO substrate material. The growth rate of the ZnO single crystal precipitate at a precipitation temperature of $830 \text{ }^\circ\text{C}$ was $0.85 \mu\text{m}/\text{min}$. The ZnO precipitate had a columnar microstructure and a developed surface with isolated pores with a density of less than 10^6 cm^{-1} and linear dimensions of up to $10 \mu\text{m}$. After chemical-mechanical polishing, the surface of the ZnO precipitate was smoothed to roughness values below 5 nm and the porosity still remained. With a decrease in the deposition temperature to $750 \text{ }^\circ\text{C}$, the growth rate increased to $1.5 \mu\text{m}/\text{min}$ and the film easily peeled off the sapphire substrate. The upper surface of the film was heterogeneous: a smooth surface had microcrystals of various shapes. The lower surface of the film had a microporous structure with the following parameters: Pores with a size of up to $10 \mu\text{m}$ and multilayer pore walls with a thickness of $1\text{--}2 \mu\text{m}$. All ZnO films were textured along $[001]$. With an increase in the deposition temperature, the epitaxial quality of the films increased.

The paper demonstrated that the ZnO deposition rates during the sputtering of hot ceramic targets were ultra-high (up to

$1.5 \mu\text{m}/\text{min}$). The obtained samples of ZnO films with a thickness of more than $50 \mu\text{m}$ can be used as a substrate material in microelectronics to manufacture light-emitting devices. Microporous films were obtained for the first time without any special surface pretreatment and template technologies. Microporous structures may be used for photonic applications: pores may be filled with various fluorescent fillers. In addition, the ZnO luminescence spectrum has two main bands: a narrow band-edge luminescence in the region of $380\text{--}390 \text{ nm}$ and a relatively wide band of visible luminescence, often characterized by a maximum of $490\text{--}530 \text{ nm}$ in the green range. Provided that pores are filled with a material with luminescence in the blue region, microporous ZnO can be a very promising source of white light.

Contribution of the authors

The authors contributed equally to this article.

Conflict of interests

The authors declare that they have no known competing financial interests or personal relationships that could have influenced the work reported in this paper.

References

1. Nakamura S., Senoh M., Mukai T. P-GaN/N-InGaN/N-GaN double-heterostructure blue-light-emitting diodes. *Japanese Journal of Applied Physics*. 1993;32(2,1A/B): 8–11. <https://doi.org/10.1143/JJAP.32.L8>
2. Nakamura S., Mukai T., Senoh M. Candela-class high-brightness InGaN/AlGaN double-heterostructure blue-light-emitting diodes. *Applied Physics Letters*. 1994;64(13): 1687–1689. <https://doi.org/10.1063/1.111832>
3. Kong X., Qiu Z., Wu L., Lei Y., Chi L. Luminescence properties of green phosphor $\text{Ca}_2\text{Ga}_2(\text{Ge}_{1-x}\text{Si}_x)\text{O}_7:y\%\text{Eu}^{2+}$ and application. *Materials*. 2023;16(10): 3671. <https://doi.org/10.3390/ma16103671>
4. Wang Q., Xie M., Fang M., ... Min X. Synthesis and luminescence properties of a novel green-yellow-emitting phosphor $\text{BiOCl}:\text{Pr}^{3+}$ for blue-light-based w-LEDs. *Molecules*. 2019;24(7): 1296. <https://doi.org/10.3390/molecules24071296>
5. Xu H., Hou X., Chen L., Mei Y., Zhang B. Optical properties of InGaN/GaN QW with the same well-plus-barrier thickness. *Crystals*. 2022;12(1): 114. <https://doi.org/10.3390/cryst12010114>
6. Gu X., Reshchikov M. A., Teke A., ... Nause J. GaN epitaxy on thermally treated c-plane bulk ZnO sub-

strates with O and Zn faces. *Applied Physics Letters*. 2004;84(13): 2268–2270. <https://doi.org/10.1063/1.1690469>

7. Sidelev D. V., Bleykher G. A., Krivobokov V. P., Koishybayeva Z. High-rate magnetron sputtering with hot target. *Surface and Coatings Technology*. 2016;308: 168–173. <https://doi.org/10.1016/j.surfcoat.2016.06.096>

8. Komlev A. A., Minzhulina E. A., Smirnov V. V., Shapovalov V. I. Influence of argon pressure and current density on substrate temperature during magnetron sputtering of hot titanium target. *Applied Physics A*. 2017;124(1): 48. <https://doi.org/10.1007/s00339-017-1458-4>

9. Graillot-Vuilecot R., Anne-Lise T., Lecas T., Cachoncinlle C., Millon E., Caillard A. Hot target magnetron sputtering process: effect of infrared radiation on the deposition of titanium and titanium oxide thin films. *Vacuum*. 2020;181: 109734. <https://doi.org/10.1016/j.vacuum.2020.109734>

10. Ismailov A. M., Nikitenko V. A., Rabadanov M. R., Emiraslanova L. L., Aliev I. S., Rabadanov M. K. Sputtering of a hot ceramic target: experiments with ZnO. *Vacuum*. 2019;168: 108854. <https://doi.org/10.1016/j.vacuum.2019.108854>

11. Tammann G. Die temperatur des beginnsinnerer diffusion in kristallen. *Zeitschrift Fur Anorganische Und Allgemeine Chemie*. 1926;157(1): 321–325. <https://doi.org/10.1002/zaac.19261570123>

12. Kiselev V. F., Kozlov S. N., Zoteev A. V. *Osnovy fiziki poverkhnosti tverdogo tela (Fundamentals of Solid Surface Physics)*. Moscow: MSU Publ., 1999. 294 p. (In Russ.)

13. Abrahams S. C., Bernstein J. L. Remeasurement of the structure of hexagonal ZnO. *Acta Crystallographica*

Section B: Structural Crystallography and Crystal Chemistry. 1969;25(7): 1233–1236. <https://doi.org/10.1107/S0567740869003876>

14. Peng C.-Y., Tian J.-S., Wang W.-L., Ho Y.-T., Chang L. Morphology evolution of a-plane ZnO films on r-plane sapphire with growth by pulsed laser deposition. *Applied Surface Science*. 2013;265: 553. <https://doi.org/10.1016/j.apsusc.2012.11.044>

15. Yang W., Wang F., Guan Z., ... Fu Y. Comparative study of ZnO thin films grown on quartz glass and sapphire (001) substrates by means of magnetron sputtering and high-temperature annealing. *Applied Sciences*. 2019;9: 4509. <https://doi.org/10.3390/app9214509>

16. Taabouche A., Bouabellou A., Kermiche F., ... Amara S. *Advances in Materials Physics and Chemistry*. 2013;3: 209. <https://doi.org/10.4236/ampc.2013.34031>

17. Kozhevnikov I. V., Buzmakov A. V., Siewert F., ... Sinn H. *Journal of Synchrotron Radiation*. 2016;23(1): 78–90. <https://doi.org/10.1107/s160057751502202x>

Information about the authors

Arsen E. Muslimov, Dr. Sci. (Phys.–Math.), Research Fellow, Federal Research Institute “Crystallography and Photonics” of the Russian Academy of Sciences (Moscow, Russian Federation).

<https://orcid.org/0000-0002-0524-7606>
amuslimov@mail.ru

Abubakar M. Ismailov, Cand. Sci. (Phys.–Math.), Associate Professor at the Department of Physical Electronics, Dagestan State University (Makhachkala, Russian Federation).

<https://orcid.org/0000-0001-6834-0560>
egdada@mail.ru

Received 02.12.2023; approved after reviewing 02.02.2024; accepted for publication 15.02.2024; published online 01.10.2024.

Translated by Irina Charychanskaya